Evaluation of RANS models for rotating flows

By A. Ooi†, B. A. Petterson Reif‡, G. Iaccarino AND P. A. Durbin

Two- and three-dimensional simulations of the flow in rotating rib-roughened ducts are carried out using several turbulence closures. One and two-equation models have been used together with the four-equation $v^2 - f$ model. In addition, a modification of this model that systematically accounts for system rotation has been used. Results show that the $v^2 - f$ model is superior to the others in predicting wall heat transfer and, for the rotating case, the modified model accurately accounts for the effect of the system frame rotation.

1. Introduction

The two-equation $k-\epsilon$ model (Launder (1974)) with the semi-empirical "wall function" approach for modeling near wall turbulence is the most widely used turbulence closure in the industrial CFD community. There are many situations in which this approach fails, such as turbulent boundary layers at low and transitional Reynolds numbers and flows with massive separation. A variety of alternative models to account for wall effects in such situations have been introduced in the last decade (Chen & Patel (1998), Patel, Rodi & Scheuerer (1985)). Many of these models incorporate *ad-hoc* "damping functions" which have been adjusted to fit experimental or computational data. An alternative approach was taken by Durbin (1991) and Durbin (1993); the standard $k - \epsilon$ formulation was extended using the elliptic relaxation methodology in order to account for nonlocal wall effects. This model ($v^2 - f$) has been used by Behnia, Parneix, Shabany & Durbin (1999), Ooi, Iaccarino & Behnia (1998), Kalitzin (1998), Parneix & Durbin (1997), and Durbin (1995) to accurately predict heat transfer and velocity profiles for various turbulent flows that are of interest to the engineering community.

Even though it has been proven to be successful in many different situations, the $v^2 - f$ model has also inherited some of the many problems associated with the standard $k - \epsilon$ model. In particular, the $k - \epsilon$ model (as with all single point closures) is unable to properly describe turbulent flows with body force effects arising from system rotation unless *ad hoc* adjustments are made to the turbulence dissipation rate (Gastki & Speziale (1993)). To partly rectify this problem, Pettersson, Durbin & Ooi (1999) proposed an extension to the original linear $v^2 - f$ model that takes into account the turbulence generated by system rotation. This model has been successfully applied to "simple" flows such as the fully developed rotating channel, duct, and the two-dimensional rotating backstep flow by Pettersson, Durbin & Ooi (1999). An improvement to this linear model has since been proposed by Pettersson (2000), who introduced a nonlinear extension that provides a fundamentally more accurate description of the flow physics than the linear formulation of Pettersson, Durbin & Ooi (1999). Even though these models have been developed from rigorous mathematics and understanding of the basic flow mechanisms,

† University of Melbourne, Australia
‡ Norwegian Defence Research Establishment, Norway

they have not yet been tested in a complex three-dimensional rotating flow environment, and the improvements over the original v^2-f model for practical engineering applications are still to be fully addressed.

2. Turbulence models

The formulation of the two-layer $k-\epsilon$, Spalart-Allmaras (SA), and standard v^2-f models has been published in many papers (see for example, Chen & Patel (1998) for the two-layer $k-\epsilon$ model, Spalart & Allmaras (1992) for the SA model, and Behnia, Parneix, Shabany & Durbin (1999) for the v^2-f model) and will not be repeated here. In the modified v^2-f model proposed by Pettersson, Durbin & Ooi (1999), the C_μ constant in the expression for eddy viscosity is a direct function of the mean strain and rotation rate tensors. The eddy viscosity is given by

$$\mu_T = \rho C_\mu^* v^2 T \tag{2.1}$$

where T is the turbulence time scale (Durbin (1993)) and C_μ^* is given by

$$C_\mu^* = C_\mu \frac{1+\alpha_2|\eta_3|+\alpha_3\eta_3}{1+\alpha_4|\eta_3|}\left(\sqrt{\frac{1+\alpha_5\eta_1}{1+\alpha_5\eta_2}}+\alpha_1\sqrt{\eta_2}\sqrt{|\eta_3|-\eta_3}\right)^{-1}. \tag{2.2}$$

In the original v^2-f model, $C_\mu^* = C_\mu$ and has a constant value of 0.22. All the α_i's in Eq. (2.2) are model constants given by

$$(\alpha_1,\alpha_2,\alpha_3,\alpha_4,\alpha_5) = \left(0.055,\frac{1}{2},\frac{1}{4},\frac{1}{5},\frac{1}{40}\right). \tag{2.3}$$

The η_i's are defined from the non-dimensional mean strain and rotation rate tensors

$$\eta_1 = S_{ik}^* S_{ik}^*, \tag{2.4}$$

$$\eta_2 = W_{ik}^* W_{ik}^* = -W_{ik}^* W_{ki}^*, \tag{2.5}$$

and

$$\eta_3 = \eta_1 - \eta_2 \tag{2.6}$$

where

$$S_{ik}^* = \frac{1}{2}T\left(\frac{\partial U_i}{\partial x_k}+\frac{\partial U_k}{\partial x_i}\right) \tag{2.7}$$

and

$$W_{ik}^* = \frac{1}{2}T\left[\left(\frac{\partial U_i}{\partial x_k}-\frac{\partial U_k}{\partial x_i}\right)+4.5\epsilon_{kim}\Omega_m\right]. \tag{2.8}$$

This modification to the expression for C_μ was obtained so that the v^2-f model "mimics" the behavior of second moment closure models in the equilibrium limit of rotating homogeneous shear flow. Additional details of this derivation can be found in Pettersson, Durbin & Ooi (1999).

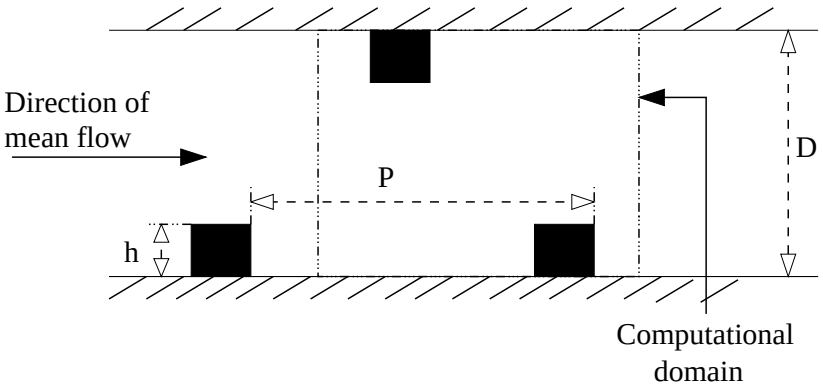

FIGURE 1. Geometry of experimental setup.

3. Test cases, mathematical model, and numerical simulations

Test cases from the 7th ERCOFTAC/IAHR Workshop on Refined Turbulence Modeling were chosen to investigate the performance of various turbulence models. Owing to the simplicity of the geometry, fully developed rotating channel flow was chosen as an ideal initial test case. Data from direct numerical simulation (DNS) of the Navier-Stokes equations are available from Kristoffersen (1993) at $Re_\tau = hu_\tau/\nu = 194$ and $R_0 = 2\Omega h/U_b = 0.1$ to check the accuracy of the simulations. Since the flow is assumed to be fully developed, periodic inflow and outflow boundary conditions were used in the calculations.

The second test case considered here is the turbulent flow in a square duct (width to height ratio of 1:1) with ribs. In the experiment, ribs are placed in a staggered arrangement on the side walls of the duct. This is illustrated in Fig. 1, which shows a side view of the experimental configuration; pitch to rib height (p/h) for the configuration used is 10 while rig height to duct height (h/D) is 0.1. The experimental measurements were taken as part of a study on the flow and heat transfer in rotating square-sectioned U-bends with rib roughened walls. The velocity field six diameters downstream of the bend exit were measured using LDA. The flow is fully developed in this straight section and unaffected by the presence of the bend. Hence, in the numerical simulations, only one portion of the duct is considered with periodic inflow/outflow boundary conditions. In the experimental facility, data from turbulent flow at rotations numbers $Ro = \Omega D/U_m$ of 0 and 0.2 with Reynolds number based on bulk velocity U_b and duct height D of 10^5 were obtained. Both flow and heat transfer data were obtained at $Ro = 0.0$, but only velocity field data were available at $Ro = 0.2$. Measurements were only taken on the symmetry plane of the duct.

The two-dimensional ($2d$) grid used in the calculations is shown in Fig. 2. It has 40,000 quadrilateral cells, and fine grid spacing was used in the vicinity of the walls to ensure the simulations are well resolved. The $2d$ simulations were carried out because the authors initially assumed that the presence of the side walls has a limited effect on the predictions at the symmetry plane where experimental data were available. Three-dimensional ($3d$) simulations carried out later showed that this assumption was incorrect; secondary flow structures have a dramatic effect on the predicted streamwise velocity at the center of the duct. The $3d$ simulations are performed using a grid that is just a spanwise extension of the $2d$ grid; it consist of 800,000 hexahedra cells.

Simulations were carried out using various turbulence models. As there is separation

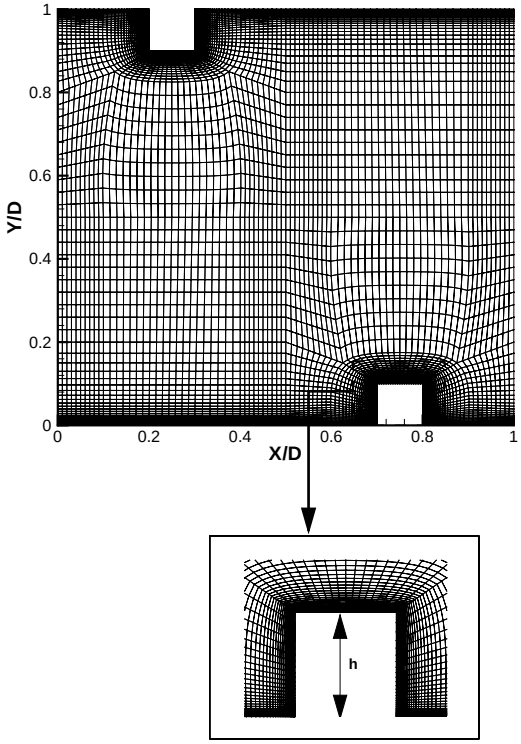

FIGURE 2. Grid used for the simulations.

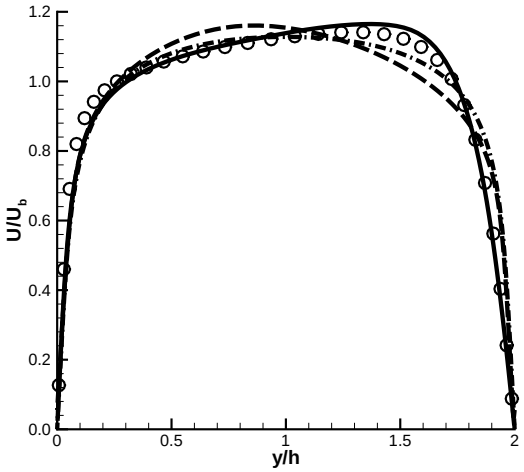

FIGURE 3. Comparison between predicted and experimental data for fully developed channel flow. • DNS data, —— $v^2 - f$ model, - - - - SA model, —·— $k - \epsilon$ model.

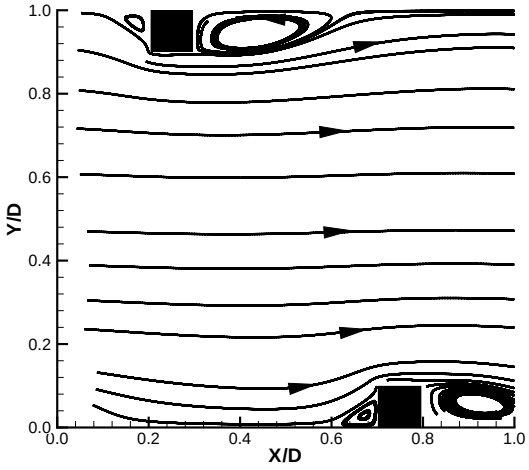

FIGURE 4. Streamlines from 2*d* calculations.

in the flow, it is expected that all turbulence models based on "wall functions" will not be able to accurately reproduce the experimental data. Hence, only turbulence models that can be integrated all the way to the wall such as two-layer $k-\epsilon$ (proposed by Chen & Patel (1998)), Spalart Allmaras (Spalart & Allmaras (1992)), v^2-f (Durbin (1991)), and the linear modified v^2-f (Pettersson, Durbin & Ooi (1999)) were tested.

4. Results

4.1. *1-d rotating channel flow*

Figure 3 shows the results from the rotating channel simulations with $R_0 = 0.1$. System rotation suppresses turbulence on one (stable) side of the channel which leads to asymmetry in the mean velocity profile. This is evident in the DNS data. As is well known, conventional eddy viscosity type closures such as the $k-\epsilon$, SA, and the original v^2-f models are relatively insensitive to system rotation and will predict a mean velocity profile that is very close to symmetric. The slight asymmetry in the SA prediction is due to the production term of the modified eddy viscosity transport equation. The production term is modeled as $\Omega_{ij}\Omega_{ij}$ whereas the production term in the $k-\epsilon$ model is just $S_{ij}S_{ij}$. Predictions using the modified linear v^2-f model accurately matche the DNS data.

4.2. 2*d rib simulations*

Figure 4 shows the flow pattern obtained with the modified v^2-f turbulence model for both the non-rotating and rotating cases. The mean flow goes from left to right, and a small separation bubble appears upstream of the rib. Downstream of the rib, another bigger separation bubble is formed. The size of the separation bubble is indicated in Fig. 5, which shows the distribution of friction coefficient C_f at the top of the duct directly downstream from the rib. The data in this figure was obtained using the modified v^2-f model, and it shows that the predicted size of the separation bubble is smaller for higher values of *Ro*. This is consistent with the experimental observation of Rothe

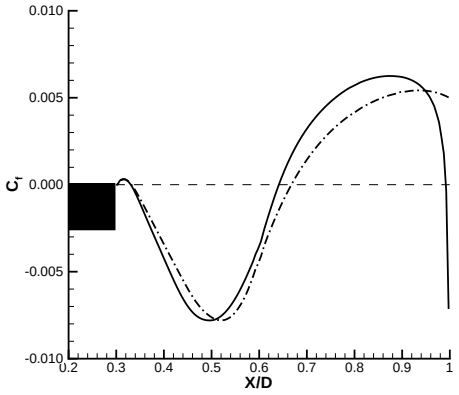

FIGURE 5. Distribution of C_f at the top of the square duct. —·— $Ro = 0.0$ and ——— $Ro = 0.2$.

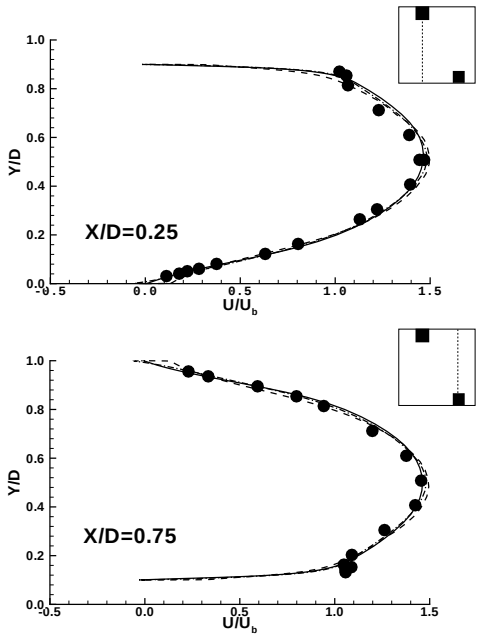

FIGURE 6. Comparison between the predicted streamwise velocity and the experimental values for $Ro = 0.0$. • Experimental data, – – – – $k-\epsilon$ model, —·— SA model and ——— v^2-f model.

(1975). In contrast, all other turbulence models tested predicted a separation length that is independent of Ro.

For the case with $Ro = 0$, a quantitative comparison of the streamwise velocity (U) with experimental data is shown in Fig. 6. This figure shows the predicted streamwise velocity with the corresponding experimental data at two streamwise locations, one station at the center of the upstream rib ($X/D = 0.25$) and the other one at the center of the downstream rib ($X/D = 0.75$). For both streamwise stations, all predictions using different turbulence models agree very well with the experimental data close to the center

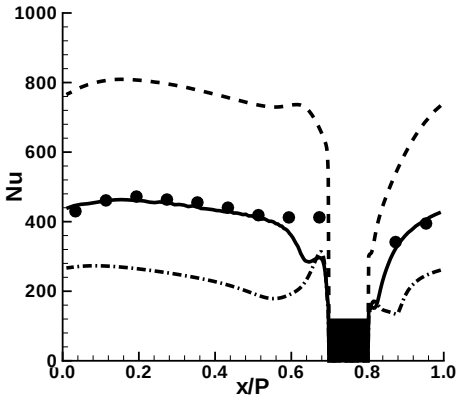

FIGURE 7. Comparison of Nu between predicted and experimental data for $Ro = 0.0$. • Experimental data, – – – – $k - \epsilon$, —·— SA and —— $v^2 - f$.

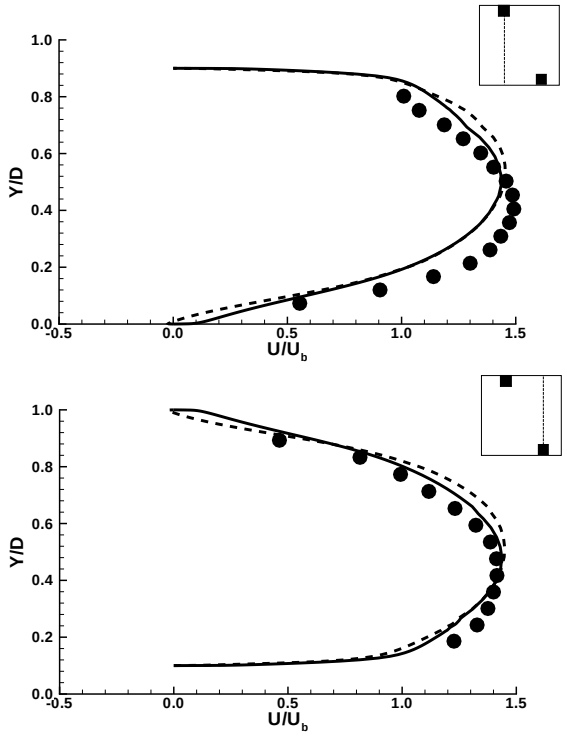

FIGURE 8. Comparison between the original and modified $v^2 - f$ model for $Ro = 0.2$. • Experimental data, – – – – original $v^2 - f$ model, —— modified $v^2 - f$ model.

of the channel. However, the predicted velocity profiles between the different turbulence models are actually very different close to the walls. This is more clearly illustrated in Fig. 7, which compares the predicted Nusselt, Nu, with the experimental data along the bottom wall of the square duct. The Nu is overpredicted by the $k - \epsilon$ model and is

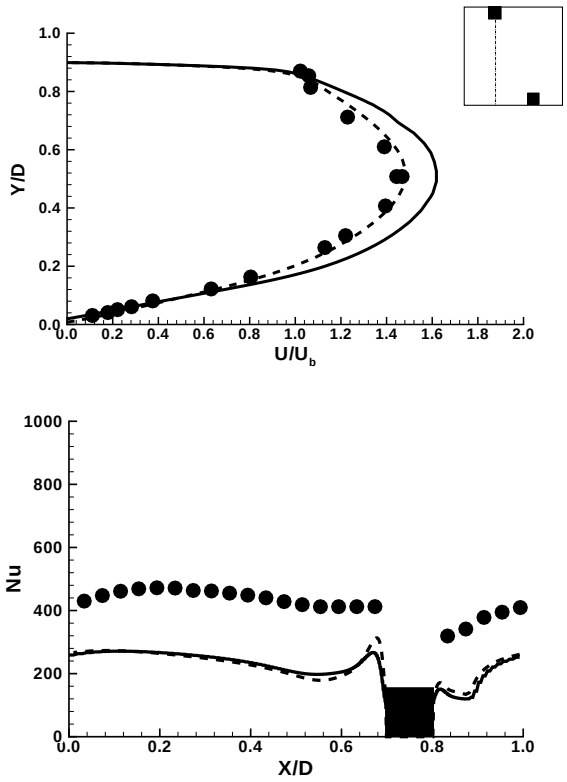

FIGURE 9. Comparison between Spalart Allmaras 2d and 3d results. • Experimental data, ---- SA (2d), —— SA (3d).

underpredicted using the SA model. Predictions using the original $v^2 - f$ model match experimental values very well.

Numerically predicted data for the case with $Ro = 0.2$ is shown in Fig. 8, which compares the data obtained using the modified and the original $v^2 - f$ model at the same streamwise stations. The modified $v^2 - f$ model changes the streamwise velocity profile such that it is a closer match to the experimental data. This indicates that the modified model more accurately models the physics of rotating flows. Unfortunately, no experimental data for Nu is available for this case. Hence, the accuracy of the modified model in predicting Nu for the rotating case is unclear.

4.3. 3d *rib simulations*

Figure 9 shows a comparison between the 2d and 3d Spalart-Allmaras model results for the case with no rotation. The Nu prediction at the bottom of the duct is similar for both the 2d and 3d cases. However, the predicted value of the streamwise velocity is remarkably different at the center of the duct. Surprisingly, the 2d prediction matches the experimental data better than the 3d prediction.

The reason for this could be due to the existence of the secondary flow structures in the 3d predictions. This is illustrated in Fig. 10, which shows the streamlines on two streamwise planes in the computational domain. The two planes are chosen to be just after the top rib at $X/D = 0.35$ and at $X/D = 0.50$, which is closer to the center of

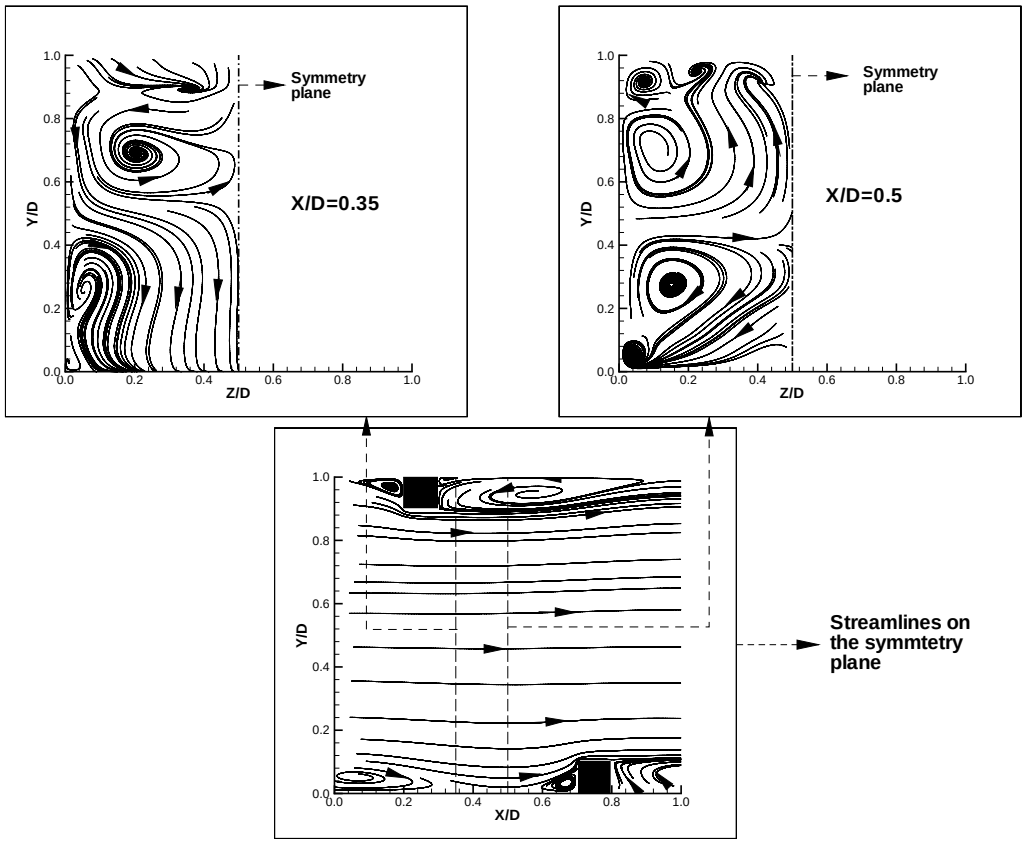

FIGURE 10. Streamlines on various downstream stations for $Ro = 0.0$.

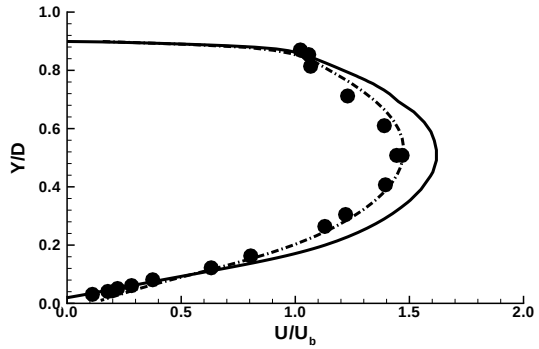

FIGURE 11. Comparison with experimental data for $Ro = 0.0$. • Experimental data, ——— SA (3d), —·— modified $v^2 - f$ (3d).

the separation bubble. It is clear that the secondary flow structures persist downstream, and mean streamwise vortices are formed in the separation bubble at $Y/D > 0.9$. Data obtained from $v^2 - f$ predictions show similar features.

Figure 11 shows how the $3d$ predictions of the velocity on the symmetry plane compares with experimental data. As discussed previously, the SA model overpredicts the velocity

on the centerline. On the other hand, the modified $v^2 - f$ model is able to correctly reproduce the velocity profile on the symmetry plane.

5. Conclusions

This paper presents results from steady-state RANS simulations of rotating and non rotating flow in a square duct. Various different turbulence models were used and, whenever possible, comparisons were made with experimental data. For $2d$ calculations, it was shown that the velocity field was well predicted with all turbulence models. For the non-rotating case, both the two-layer $k - \epsilon$ and Spalart-Allmaras models give heat transfer predictions that are very different from the experimental data. Both variations of the $v^2 - f$ models tested give very good heat transfer distribution, indicating the superior near-wall modeling using the elliptic relaxation methodology. For the $2d$ rotating case, the modified $v^2 - f$ model gives a velocity profile that is closer to the experimental values than the original $v^2 - f$ model.

Three-dimensional simulations were also carried out and the differences between the $2d$ and $3d$ results were reported. For the non-rotating case, the predicted velocity profile from the $2d$ calculations using the SA model were actually closer to the velocity profile measured in the experiments. This is especially evident at the center of the square duct. One possible explanation is that the secondary flow structures which exist in the $3d$ calculations are very complicated and not properly modeled by the SA model. On the other hand, $3d$ calculations using the modified $v^2 - f$ model produce a velocity profile that matches the experimental values.

REFERENCES

Behnia, M., Parneix, S., Shabany, Y. & Durbin, P. A. 1999 Numerical study of turbulent heat transfer in confined and unconfined impinging jets. *Int. J. Heat and Fluid Flow.* **20**, 1-9.

Chen, H. C. & Patel, V. C. 1988 Near-wall turbulence models for complex flows including separation *AIAA J.* **26**(6), 641-648.

Durbin, P. A. 1991 Near-wall turbulence closure modeling without "damping functions". *Theoret. Comput. Fluid Dyn.* **3**, 1-13.

Durbin, P. A. 1993 A Reynolds stress model for near-wall turbulence. *J. Fluid Mech.* **249**, 465-498.

Durbin, P. A. 1995 Separated flow computations with the $k - \epsilon - v^2$ model. *AIAA J.* **33**(4), 659-664.

Gatski, T. B. and Speziale, C. G. 1993 On explicit algebraic stress models for complex turbulent flows. *Int. J. Fluid Mech.* **254**, 59-78.

Kalitzin, G. 1998 An implementation of the $v^2 - f$ model with application to transonic flows. *Annual Research Briefs*, Center for Turbulence Research, NASA Ames/Stanford Univ. 171-184.

Kristoffersen, R. & Andersson, H. I. 1993 Direct simulations of low-Reynolds-number turbulent flow in a rotating channel. *J. Fluid Mech.* **256**, 163-197.

Launder & Spalding 1974 The numerical computation of turbulent flows. *Comp. Methods Appl. Mech. Engr.* **3**, 269-289.

Ooi, A., Iaccarino, G. & Behnia, M. 1998 Heat transfer predictions in cavities.

Annual Research Briefs, Center for Turbulence Research, NASA Ames/Stanford Univ. 185-196.

Parneix, S. & Durbin, P. 1997 Numerical simulation of 3D turbulent boundary layers using the V2F model. *Annual Research Briefs*, Center for Turbulence Research, NASA Ames/Stanford Univ. 135-148.

Patel, V. C., Rodi, W. & Scheuerer, G. 1985 Turbulence models for near-wall and low Reynolds number flows:a review. *AIAA J.* **23**(9), 1308-1319.

Pettersson Reif, B. A., Durbin, P. & Ooi, A. 1999 Modeling rotational effects in eddy-viscosity closures. 1999 *Int. J. Heat and Fluid Flow.* **20**, 563-573.

Pettersson Reif, B. A. 2000 A nonlinear eddy-viscosity model for near-wall turbulence. *AIAA 2000-135.*

Rothe, P. H. 1975 The effects of system rotation on separation, reattachment and performance in two-dimensional diffusers.*Stanford University Dissertation, Department of Mechanical Engineering.*

Spalart, P. R. & Allmaras, S. R. 1992 A one-equation turbulence model for aerodynamic flows. *AIAA 92-0439.*